Modelling heat and mass transfer in bread baking with mechanical deformation

Vincent Nicolas, Patrick Salagnac, Patrick Glouannec, Jean Pierre Ploteau, Vanessa Jury, Lionel Boillereaux

Modelling heat and mass transfer in bread baking with mechanical deformation

V Nicolas[a,b], P Salagnac[b], P Glouannec[a], J-P Ploteau[a], , V Jury[c], L Boillereaux[c]

[a]Laboratoire d'Ingénierie des MATériaux de Bretagne – Equipe Thermique et Energétique, Université Européenne de Bretagne, B.P. 92116, 56321 Lorient Cedex

[b]Laboratoire des Sciences de l'Ingénieur pour l'Environnement, Université de La Rochelle, Pôle Sciences et Technologie - Av. M. Crépeau, 17042 La Rochelle Cedex 1

[c]Laboratoire de Génie des Procédés, Environnement, Agroalimentaire, ONIRIS, rue de la Géraudière, B.P. 82225, 44322 Nantes Cedex 3

E-mail : patrick.glouannec@univ-ubs.fr - vincent.nicolas@univ-ubs.fr

Abstract. In this paper, the thermo-hydric behaviour of bread during baking is studied. A numerical model has been developed with Comsol Multiphysics© software. The model takes into account the heat and mass transfers in the bread and the phenomenon of swelling. This model predicts the evolution of temperature, moisture, gas pressure and deformation in French "baguette" during baking. Local deformation is included in equations using solid phase conservation and, global deformation is calculated using a viscous mechanic model. Boundary conditions are specified with the sole temperature model and vapour pressure estimation of the oven during baking. The model results are compared with experimental data for a classic baking. Then, the model is analysed according to physical properties of bread and solicitations for a better understanding of the interactions between different mechanisms within the porous matrix.

1. Introduction

In France, 30 000 bakers produce bread, which generates a considerable energy consumption in the French food sector. An improvement of the energy efficiency of the oven would make it possible to reduce the energy request for this sector and consequently the CO_2 emissions. Before the optimization phase, it is necessary to evaluate the energy needs of the product. This stage needs an increased knowledge and a modeling of the transfer mechanisms in the product during baking, here, a porous medium: bread. Several fundamental complex physical processes are coupled during bread baking like heat and mass transfers, evaporation of water, volume expansion, gelatinization of starch, formation of the porous structure, crust formation, surface browning reaction, Different mathematical models of bread baking process can be found in the scientific literature [1][2]. However, these models do not take into account the whole of transport process and the coupling with physicochemical mechanisms. It appears interesting to build a complete model to understand the interactions between the different phenomena inside the product and between the product and the baking processes.

The first part of this work presents the mathematical model. This model is then solved using a finite element method. A classic baking of a French "baguette" is simulated in a first time and compared with experimental data. In a second time, the model is tested with different solicitations. At the end of this work, results are analyzed and discussed.

2. Physical mechanisms

Bread is a complex medium in which occur many physical phenomena, during baking (Figure 1, Figure 2). Dough is made up of carbon dioxide bubbles linked to the raising [3][4]. Initially the bubbles are isolated from each other; there is no transfer of gas. When the bubbles grow with the release of CO_2 and the temperature increases, they come into contact and the gas transfer becomes possible [5]. Bread swelling induces an increase of porosity. This is due to yeast fermentation that releases carbon dioxide, which creates a pressure increase at the beginning of cooking. The fermentation rate increased by 8%, for each additional degree, starting from 20°C until 40°C. From 40°C, the activity decreased and then stopped at 50°C. Rheological properties have a significant effect on the deformation, gelatinization happens at about 60°C and the dough turns into crumbs [6]. With the appearance of the crust, the deformation is constrained due to the solid structure. The browning is the last phenomenon that occurs during cooking; this phenomenon will not be possible if there was no "blow steam" at the beginning of cooking. The coupling of all these phenomena is complex and dependent on the other one.
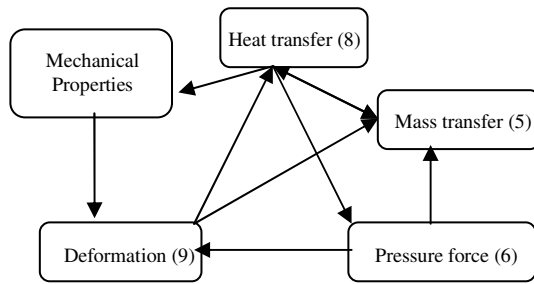

Figure 1. Interaction between the different phenomena occurring during the baking of bread.
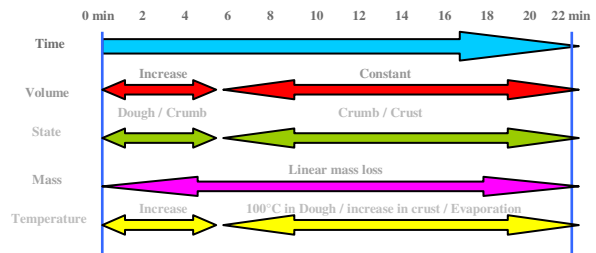

Figure 2. Phenomena evolution.

3. Physical model

The present study deals with the ovens used for the making of traditional "French bread". The baking is done with hot air (natural convection), infrared radiation and direct conduction (Figure 3). The creation of a knowledge model allows the modeling of all the phenomena occurring during baking (Figure 3). The transfer of heat and mass, the appearance of porosity, the swelling and the physico-chemical phenomena are the main phenomena occurring during baking. Therefore, the physical model includes the conservation equations of energy and mass to evaluate the water content, pressure, porosity and temperature [1]. It also includes deformation terms to evaluate the velocity fields.
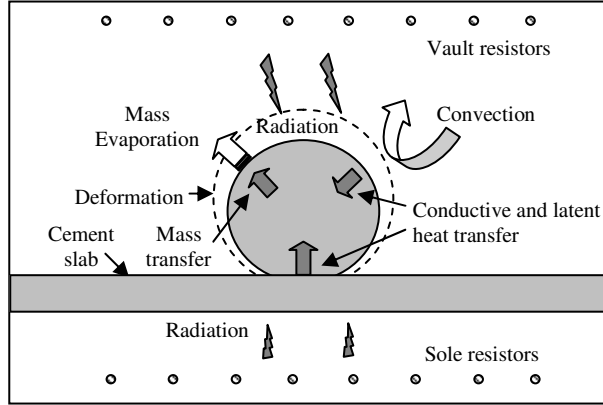
Figure 3. Transfers of mass and heat during baking of bread.

3.1. Mass conservation

In this model, four constituents are considered: liquid water (l), vapour water (v), carbon dioxide (CO_2) gas and solid (s) phase. The equations of mass conservation are written as Bird et al. (2002)[7]. Mass flux $\vec{n}$ can be described by two phenomena. The first is a convective flux which depends on the mean filtration velocity. The mean filtration velocity of each component is expressed by Darcy's law as a function of pressure gradient. The second phenomenon, only for gas, comes from Fick's law. It's a diffusive flux which depends on the mass fraction gradient in the mixture [8]. For each gas and liquid flux, deformation had to be taken into account in the flow [9][10].

Liquid water conservation
$$\frac{\partial \rho_l^a}{\partial t} + \vec{\nabla} \cdot \left(\vec{n}_l + \rho_l^a \vec{V} \right) = -K_v \tag{1}$$

Vapor water conservation
$$\frac{\partial \rho_v^a}{\partial t} + \vec{\nabla} \cdot \left(\vec{n}_v + \rho_v^a \vec{V} \right) = K_v \tag{2}$$

Carbon dioxide gas conservation
$$\frac{\partial \rho_{co_2}^a}{\partial t} + \vec{\nabla} \cdot \left(\vec{n}_{co_2} + \rho_{co_2}^a \vec{V} \right) = K_{co_2} \tag{3}$$

Solid conservation
$$\frac{\partial \rho_s^a}{\partial t} + \vec{\nabla} \cdot \left(\rho_s^a \vec{V} \right) = 0 \tag{4}$$

with ρ_i^a, the apparent density of the constituent i and K_i, the phase change rate.

3.2. Moisture content equation W (dry basis)

By adding liquid and vapor water mass conservation equation, the moisture content equation is obtained. Liquid water transfer with temperature gradient is neglected. Liquid and vapor water unsteady terms are explained as follow:

With $\dfrac{\partial \rho_l^a}{\partial t} = \zeta_1 \dfrac{\partial W}{\partial t} - \zeta_2 \dfrac{\partial \varepsilon_g}{\partial t}$ and $\dfrac{\partial \rho_v^a}{\partial t} = \beta_1 \dfrac{\partial T}{\partial t} + \beta_2 \dfrac{\partial W}{\partial t} + \beta_3 \dfrac{\partial \varepsilon_g}{\partial t}$ (5)

We obtain:

$$(\zeta_1 + \beta_2)\frac{\partial W}{\partial t} + (-\zeta_2 + \beta_3)\frac{\partial \varepsilon_g}{\partial t} + \beta_1 \frac{\partial T}{\partial t} + \vec{\nabla} \cdot \left(\begin{array}{c} \left(D_l^W + D_v^W\right)\vec{\nabla}W + D_v^T \vec{\nabla}T + D_v^{P_g}\vec{\nabla}P_g \\ + \left(\rho_l^a + \rho_v^a\right)\vec{V} \end{array} \right) = 0 \tag{6}$$

$\zeta_1, \zeta_2, \beta_1, \beta_2, \beta_3$ are model coefficients and $D_l^W, D_v^W, D_v^T, D_v^{P_g}$ mass diffusion coefficients. All coefficients are explained in appendix.

3.3. Pressure equation P_g

Pressure has an important place during bread baking. The pressure gradient is the driving of the mass flows. Deformation is principally due to overpressure in core. Total pressure equation of the gaseous phase P_g is obtained from the mass conservation equation of CO_2 [8].

$$\frac{\partial P_g}{\partial t} = \frac{1}{\gamma_3}\left[-\vec{\nabla}\cdot\left(D_{CO_2}^W\vec{\nabla}W + D_{CO_2}^T\vec{\nabla}T + D_{CO_2}^{P_g}\vec{\nabla}P_g + \rho_{CO_2}^a\vec{V}\right) - \gamma_1\frac{\partial T}{\partial t} - \gamma_2\frac{\partial W}{\partial t} - \gamma_4\frac{\partial \varepsilon_g}{\partial t} + K_{CO_2}\right] \tag{7}$$

$\gamma_1, \gamma_2, \gamma_3, \gamma_4$ are model coefficients and $D_{CO_2}^W$, $D_{CO_2}^T$, $D_{CO_2}^{P_g}$ mass diffusion coefficients.

3.4. Gas fraction equation ε_g

The deformation of the bread during baking induces a local deformation. The displacement of the solid matrix corresponds to an increase of porosity at the center of the product. Local gas fraction equation is calculated with the solid conservation equation. Gas fraction allows to calculate porosity depending on solid matrix deformation and water content.

$$\left(\frac{\rho_s^i}{\rho_l^i}\zeta_2 - \rho_s^i\right)\frac{\partial \varepsilon_g}{\partial t} + \vec{\nabla}\cdot\rho_s^a\vec{V} = \frac{\rho_s^i}{\rho_l^i}\zeta_1\frac{\partial W}{\partial t} \tag{8}$$

3.5. Heat transfer equation

Temperature in bread is calculated using transient heat transfer equation. A reading of energy balance shows heat transfers through convection, displacement of the porous matrix, conduction and phase change [8].

$$\rho C_p\frac{\partial T}{\partial t} + \left[\begin{pmatrix}\left(D_l^W\vec{\nabla}W\right)C_{p;l} \\ \left(D_v^W\vec{\nabla}W + D_v^T\vec{\nabla}T + D_v^{P_g}\vec{\nabla}P_g\right)C_{p;v} \\ \left(D_{CO_2}^W\vec{\nabla}W + D_{CO_2}^T\vec{\nabla}T + D_{CO_2}^{P_g}\vec{\nabla}P_g\right)C_{p;CO_2}\end{pmatrix} + \rho C_p\vec{V}\right]\cdot\vec{\nabla}T$$

$$= \vec{\nabla}\cdot\left(\lambda\vec{\nabla}T\right) + \left(\zeta_1\frac{\partial W}{\partial t} - \zeta_2\frac{\partial \varepsilon_g}{\partial t} + \vec{\nabla}\cdot\left(D_l^W\vec{\nabla}W + \rho_l^a\vec{V}\right)\right)L_v \tag{9}$$

with ρ, the bread density, C_p the equivalent heat capacity, λ the thermal conductivity and L_v the water latent heat. Phase change rate is deduced from the liquid water conservation equation. In this article, the heat transfer in sole is modeled and writes, the variable is named T_s.

3.6. Deformation

To take into account the swelling of the bread, Vanin (2010) [5] considers bread like a Newtonian fluid (Bird et al. (2002)[7]. So, momentum conservation equation is used to calculate swelling velocity $\vec{V}$.

$$\rho\frac{\partial \vec{V}}{\partial t} + \vec{V}\left(\frac{\partial \rho_l^a}{\partial t} + \frac{\partial \rho_s^a}{\partial t} + \frac{\partial \rho_{co_2}^a}{\partial t} + \frac{\partial \rho_v^a}{\partial t}\right) + \vec{\nabla}\cdot\left(\rho\vec{V}\cdot\vec{V} + P_g\overline{\overline{\delta}} + \eta\left(\vec{\nabla}\vec{V} + \left(\vec{\nabla}\vec{V}\right)^T\right) - \frac{2\eta}{3}\left(\vec{\nabla}\cdot\vec{V}\right)\vec{I}\right) = 0 \tag{10}$$

with η, the bread viscosity and $\vec{I}$, the identity matrix.

3.7. Boundary conditions

3.7.1. Air/product interface

Evaporated mass flux (F_m) is equal to the sum of liquid water and vapor flux.

$$-\vec{n}\cdot\left(\vec{n}_l + \vec{n}_v\right) = F_m \tag{11}$$

with:

$$F_m = k_m \left(\frac{P_t M_v}{R T_{film}} \right) \ln \left(1 + \left(\frac{P_{v,surf} - P_{v,\inf}}{P_t - P_{v,surf}} \right) \right) \text{ and } k_m = \frac{h_c}{\rho C_p Le^{2/3}} \tag{12}$$

Atmospheric pressure is considered for gas pressure and deformation equation.

$$P_g = P_{atm} \tag{13}$$

Calculated velocity is applied for gas fraction equation.

$$-\vec{n} \cdot \left(\rho_s^a \vec{V} \right) = \rho_s^a \vec{V}_{surf} \tag{14}$$

Convective and irradiative heat transfers are considered. The surfaces are supposed grey body. Irradiative heat transfer is different if the product has a sole or vault heat irradiation.

$$-\vec{n} \cdot \left(\lambda \vec{\nabla} T + \vec{n}_l L_v \right) = h_c (T_{air} - T) + \varepsilon \left[G - \sigma T^4 \right] \tag{15}$$

3.7.2. Sole interface

There is no mass transfer at the sole contact, velocity is set to zero. An equivalent thermal contact resistance R_c is used to simulated conductive flux.

4. Numerical model

The previous model has been implemented in a computer code by finite element method (Comsol ©). A 2D geometry is specified on Figure 4. A triangular mesh comprising 4481 elements was selected. Formalism ALE (Arbitrary Lagrangian-Eulerian formulation) is used to take into account the deformation of bread. States variables calculated are temperature T, moisture content W, gas pressure P_g, gas fraction ε_g, sole temperature T_s and mechanical velocities (u,v). Each states variable is obtained by a differential partial equation. The set of equations are coupled. The initial geometry and the Mesh are presented Figure 4. The dough (2) is modeled with a height of 3.2 cm, a width of 5 cm and a length of 53 cm. The sole (1) is 2 cm of height and a width of 5. This time dependant study is solved with a direct solver. All the variables are saved every 10 seconds for each variable calculated.
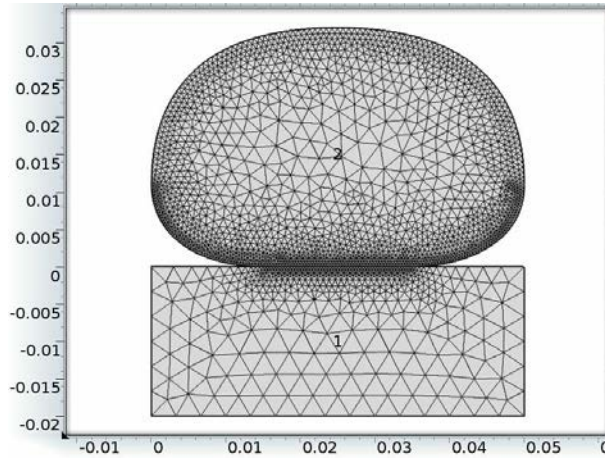

Figure 4. Mesh geometry.

4.1. Results and discussion

4.2. Classical baking

Experimental conditions measured during a real baking are imposed [11]. The air temperature is equal to 200°C and the infrared irradiation received by the product is not constant. The dough at a temperature of 25°C, a moisture content of 0,781(db), and a gas fraction of 0,649 is introduced in the

oven. The sole surface temperature is 240°C and initial gradient sole temperature exists at the beginning. The first test is simulated without scarification and blow of steam.
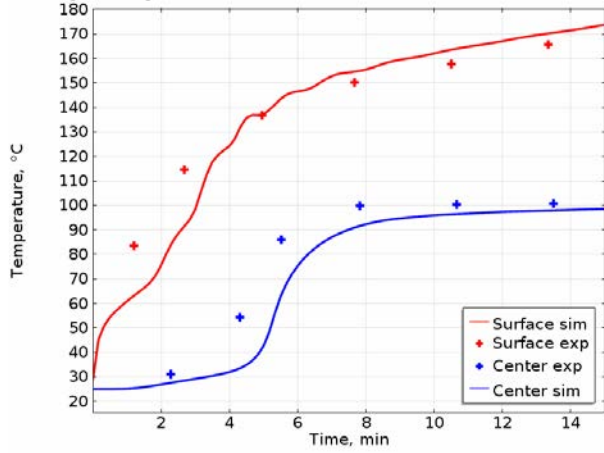

Figure 5. Simulated and experimental temperature evolutions on surface and on center of bread.

Figure 6. Simulated and experimental mass evolutions.

For the temperature evolutions (Figure 5), two points are measured: surface and center. At the surface of the bread, the temperature increases continuously except for high irradiations. When we reached significant levels of irradiation, experimental tests are regulated. This explains the difference between the simulated and the experimental curve corresponding to an average of several tests. Outside this area, the simulations are similar to experimental data. Bread center increase until 100°C and stay at this value. The simulated mass loss (Figure 6) corresponds to the experimental evolution.
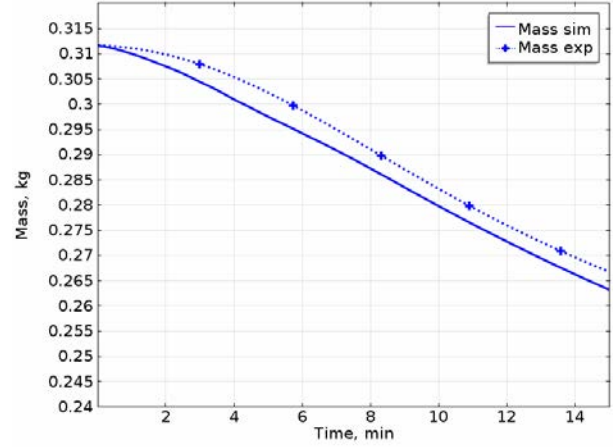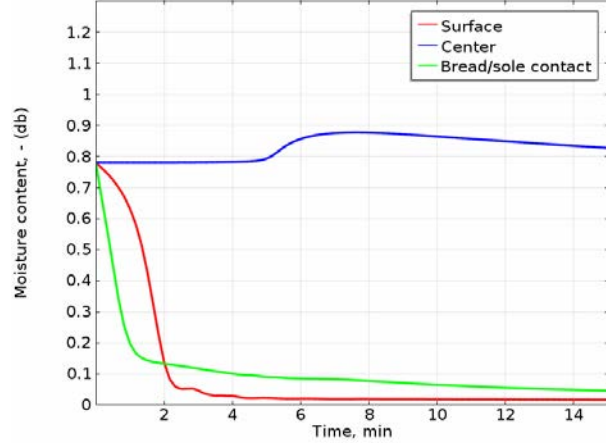

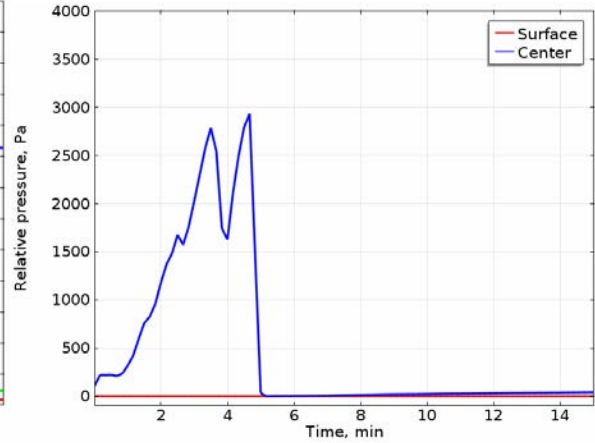**Figure 7.** Simulated moisture content on surface, center and on contact with sole.

Figure 8. Simulated relative gas pressure on surface and on center.

Figure 7 presents the simulated local moisture contents. They are consistent with the data found in scientific literature [12]. At the bread center, moisture content stays at initial value and increases slightly. As the opposite, the surface moisture content decreases until the equilibrium moisture level value. Figure 8 presents the simulated gas pressure. It increases in the center of the bread during the five first minute. Before 55°C, gas mass fluxes are held to zero due to the closed porosity of dough. Pressure increases due to this phenomenon. After 55°C, gas fluxes are freed with pore opening and pressure decreases to atmospheric pressure. With pore opening temperature and moisture increase in the center, this is the evaporation-condensation phenomenon. At the surface, the pressure is constant and equal to the atmospheric pressure.
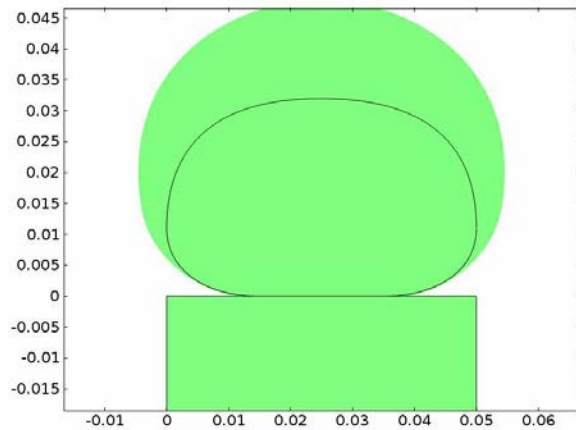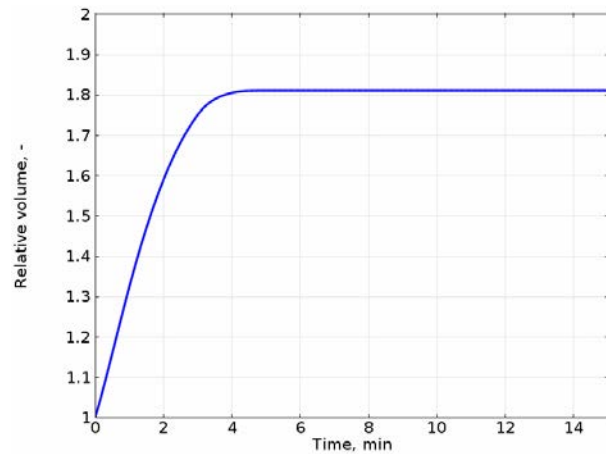
Figure 9. Simulated deformation.

Figure 10. Simulated porosity on surface and on center.

Experimentally, it is difficult to evaluate the volume of bread. The volume increases very rapidly during the first two minutes of cooking. Experimentally, the volume increases between 60% and 100% of the initial volume. This simulation (Figure 9, Figure 10) obtains a value of 82% which is consistent with reality.

4.3. Energy analysis and sensitivity study

Three heat exchanges occur during baking: conductive with sole, convective with air and radiative with vault and wall. By integrating the heat flux applied to the boundary conditions, energy can be evaluated. For conventional cooking, the energy calculated by the model is equal to 180 000 J. Convective part is evaluated at 14%, conduction at 19% and the most part are irradiative heat transfer with 67% (Figure 11).
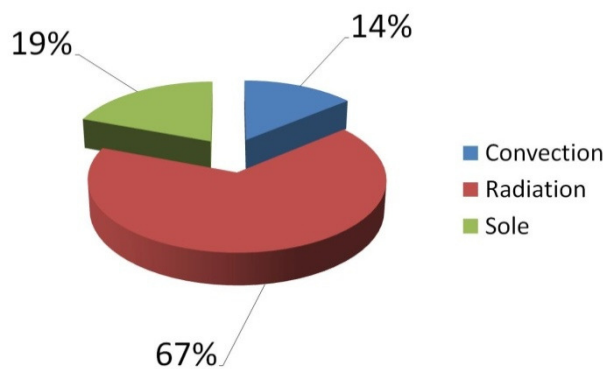

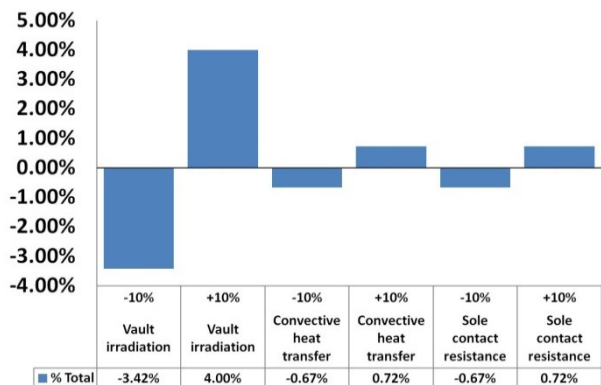**Figure 11.** Energy part of heat transfer.

Figure 12. Energetic impact of radiative, convective and conductive heat transfers.

A sensitivity study (Figure 12) with a variation of +/- 10 % of these three thermal solicitations is realized, vault irradiation G, convective heat transfer hc and sole contact resistance Rc. Energy impact is analysed and it shows an important sensitivity with vault irradiation.

5. Conclusion

A porous multiphase mathematical model is used to simulate French bread baking. Temperature, mass, moisture content, gas pressure, gas fraction and deformation are calculated in this model. Experimental boundary conditions are used for simulation and sole is simulated to have real baking conditions. Simulations are in good agreement with experimental data for mass, temperature and

deformation. To optimise energy consumption, it is important to know the repartition and the quantity of energy used by cooking. An energy analysis has been carried out and shows that radiation heat transfer represents the most part of energy consumption.

6. Acknowledgements

7. Appendix

$$\beta_1 = \frac{\varepsilon M_v (1-S)}{RT}\left[\frac{\partial P_v}{\partial T} - \frac{P_v}{T}\right]; \beta_2 = \frac{\varepsilon M_v (1-S)}{RT}\left[\frac{\partial P_v}{\partial W}\right]; \beta_3 = \frac{M_v P_v}{RT}; \gamma_1 = \gamma_3\left[\frac{P_v - P_g}{T} - \frac{\partial P_v}{\partial T}\right];$$

$$\gamma_2 = -\gamma_3\left[\frac{\partial P_v}{\partial W} - \frac{\rho_s(P_g - P_v)}{\rho_l^i \varepsilon(1-S)}\right]; \gamma_3 = \frac{\varepsilon M_{CO_2}(1-S)}{RT}; \gamma_4 = \frac{P_{CO_2} M_{CO_2}}{RT}; \zeta_1 = \frac{\rho_s^a \rho_l^i}{\left(\rho_l^i + W\rho_s^i\right)}; \zeta_2 = \frac{W\rho_s^i \rho_l^i}{\left(\rho_l^i + W\rho_s^i\right)}$$

8. References

[1]   Zhang J, Datta AK, Mukherjee S 2005 Transport processes and large deformation during baking of bread *AIChE Journal* **51(9)** 2569–2580
[2]   Jefferson DR, Lacey AA, Sadd PA 2007 Crust density in bread baking: Mathematical modelling and numerical solutions *Applied Mathematical Modelling* **31(2)** 209-225
[3]   Chiotellis E and Campbell G.M. 2003 Proving of Bread Dough I: Modelling The Evolution of the Bubble Size Distribution *Food and Bioproducts Processing* **81(3)** 194–206
[4]   Chiotellis E and Campbell G.M. 2003 Proving of Bread Dough II: Measurement of Gas Production and Retention *Food and Bioproducts Processing* **81(3)** 207–216
[5]   Vanin FM 2010 Formation de la croûte du pain en cours de cuisson, propriétés rhéologiques et séchage en surface: une approche expérimentale et de modélisation *Thèse de doctorat* Institut des Sciences et Industries du vivant et de l'Environnement (AgroParisTech)
[6]   Rouillé J, Chiron H, Colonna P, Della Valle G, Lourdin D 2010 Dough/crumb transition during French bread baking *Journal of Cereal Science* **52(2)** 161–169
[7]   Bird RB, Stewart WE, Lightfoot EN 2002 *Transport phenomena* Wiley
[8]   Salagnac P, Glouannec P, Lecharpentier D 2004 Numerical modeling of heat and mass transfer in porous medium during combined hot air, infrared and microwaves drying *International Journal of Heat and Mass Transfer* **47(19-20)** 4479–4489
[9]   Cáceres Salazar G 2006 Modélisation du séchage d'un milieu poreux saturé déformable : prise en compte de la pression du liquide *Thèse de doctorat* Ecole Nationale Supérieure d'Arts et Métiers
[10]   Zhang J and Datta AK 2006 Mathematical modeling of bread baking process *Journal of Food Engineering* **75(1)** 78–89
[11]   Ploteau J-P, Magueresse A, Nicolas V, Glouannec P 2012 Caractérisation multiphysique de la cuisson de baguette *Société française de thermique* 747–754
[12]   Wagner M, Lucas T, Le Ray D, Trystram G 2007 Water transport in bread during baking *Journal of Food Engineering* **78(4)** 1167–1173